



UNIVERSITY OF LEEDS

This is a repository copy of *Sampling from single cells*.

White Rose Research Online URL for this paper:

<http://eprints.whiterose.ac.uk/124246/>

Version: Accepted Version

Article:

Actis, P orcid.org/0000-0002-7146-1854 (2018) Sampling from single cells. *Small Methods*, 2 (3). 1700300.

<https://doi.org/10.1002/smtd.201700300>

© 2018 WILEY-VCH Verlag GmbH & Co. KGaA, Weinheim. This is the peer reviewed version of the following article: Actis, P (2018) Sampling from single cells. *Small Methods*, 2 (3), which has been published in final form at <https://doi.org/10.1002/smtd.201700300>. This article may be used for non-commercial purposes in accordance with Wiley Terms and Conditions for Self-Archiving.

Reuse

Items deposited in White Rose Research Online are protected by copyright, with all rights reserved unless indicated otherwise. They may be downloaded and/or printed for private study, or other acts as permitted by national copyright laws. The publisher or other rights holders may allow further reproduction and re-use of the full text version. This is indicated by the licence information on the White Rose Research Online record for the item.

Takedown

If you consider content in White Rose Research Online to be in breach of UK law, please notify us by emailing eprints@whiterose.ac.uk including the URL of the record and the reason for the withdrawal request.



eprints@whiterose.ac.uk
<https://eprints.whiterose.ac.uk/>

Sampling from single cells

Paolo Actis

School of Electronic and Electrical Engineering, University of Leeds, Woodhouse Lane, Leeds
LS2 9JT, United Kingdom

p.actis@leeds.ac.uk

Abstract

The cell is the fundamental unit of biology. Major methodological advances in engineering and molecular biology have enabled the ‘omics analysis of individual cells and supported biologist in understanding the deepest difference between health and disease. These advancements were based on the assumption that a single-cell needs to be lysed or fixed before any in-depth analysis can be performed. This review aims to paint a picture of innovative methods used for extracting the content of living cells without affecting their viability.

These novel methods are now empowering the biological community to repeatedly interrogate a single cell over time, thus giving a dynamic representation of the cell’s ‘omics rather than a snapshot at a particular time point.

Introduction

The cell is the fundamental unit of biology and the building block of life. Since the invention of optical microscopy, scientists have studied the morphology of individual cells but only very recently has the scientific community started to fully appreciate the fundamental molecular diversity of morphologically indistinguishable cells.

In multicellular organisms, physiology stems from an intricate and dynamic balance of single-cell activity and intercellular connections which gets disrupted by the emergence of disease that may give raise to abnormal cell types and states. Scientists have been interested in identifying these cell types and states for many years and preliminary classifications have been made possible only very recently thanks to major methodological breakthroughs in engineering

and molecular biology^[1]. Microfluidics has enabled the parallel analysis of tens of thousands of cells^[2], while novel molecular biology techniques have allowed the analysis of the minute amount of genetic material contained in one single cell^[3-5] and sophisticated bioinformatics analysis disentangled statistically significant results from measurement bias^[6]. In 2017, tens of thousands of single cells can be assayed simultaneously to measure their transcriptional profile at a cost that is very rapidly decreasing^[7, 8].

These advances in single-cell technologies are now culminating in one the most ambitious projects in human biology the “Human Cell Atlas” (<https://www.humancellatlas.org/>) which aims to create a complete reference map for all human cells^[9].

Several recent reviews have comprehensively summarized the state of the art of the field, including the current state of the science of single-cell genome sequencing^[6], the emergence of single-cell metabolomics^[10], advances and application of single-cell sequencing technologies^[11] and the computational challenges associated with analysis of single-cell transcriptomics data^[12].

This review aims to paint a picture of the methods used for extracting the content of living cells without affecting their viability (Figure 1). These methods are challenging the assumption that a single cell needs to be lysed or fixed before any in-depth analysis can be performed.

Such technological advances, although at very early stages, are now enabling the biological community to study the ‘omics of single cells with unprecedented resolution. A single living cell can be repeatedly interrogated over time, thus giving a dynamic representation of the genotype of interest rather than a snapshot at a particular time point. The development of these methods is driving the further refinement of sample preparation methods for downstream analysis of the extracted content. Next-generation sequencing has now been applied to sequence just a fraction of a cell’s RNA^[13] and the extracted contents also can be analysed with electron microscopy^[14] or advanced mass spectrometry techniques^[15, 16].

This review will describe and critically assess the benefits and limitations of 3 different methods employed to extract material from living cells (Figure 1):

1. Atomic force microscopy (AFM)
2. Nanopipette
3. Nanostraws

Methods based on carbon nanotubes^[17, 18], nanowires^[19], and nanofountain probes^[20] that could potentially be applied for the extraction of contents of living cells have been reported in literature. These methods, however, will not be discussed in this review because their ability to carry out such experiments has not been fully demonstrated.

Four ways for removing cell contents

Cao *et al.* used 150-nm-diameter alumina nanostraws combined with electroporation to extract cellular contents for analysis. This method complements nanobiopsy, fluid force microscopy, and carbon nanotube endoscopy.

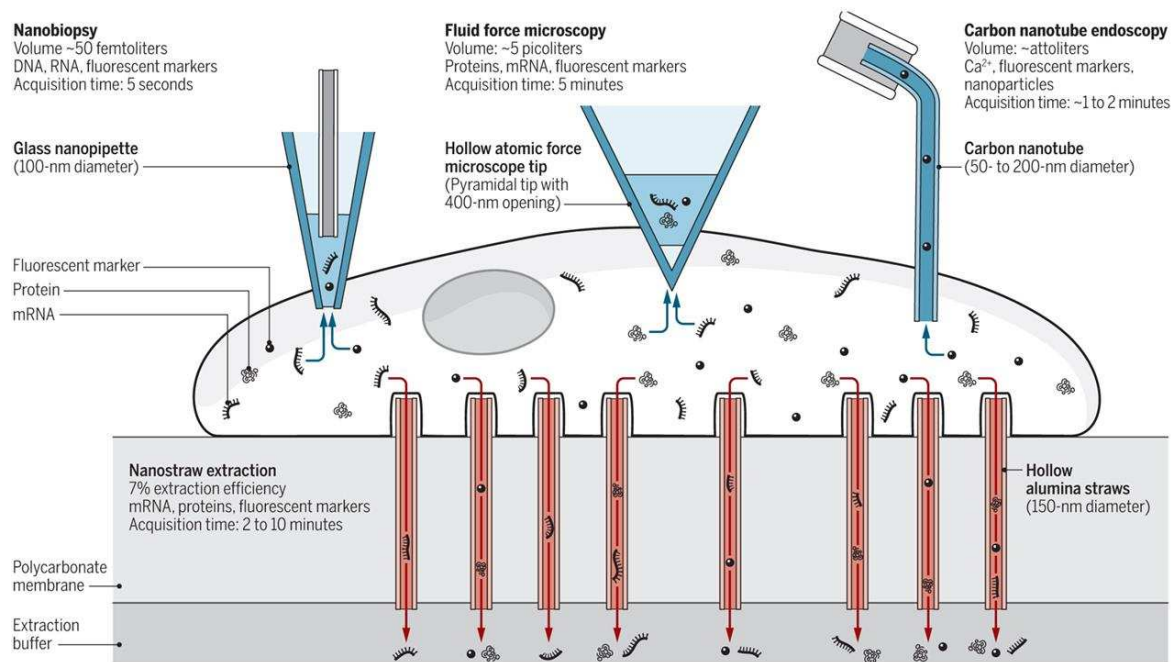


Figure 1. Schematic representation of methods for removing cell contents. Reprinted with permission from AAAS[21]

1. AFM-based Methods

1.1 DiElectrostatic NanoTweezers (DENT)

Wickramasinghe's group pioneered the use of Atomic Force Microscopy (AFM) to extract nucleic acids, in particular RNA, from individual living cells.

In 2009, his group modified a standard AFM probe to comprise a dielectrophoretic nanotweezer (DENT)^[22]. The authors first deposited a thin layer of SiO₂ on a highly-doped silicon AFM probe to isolate its conductive core and then a thin layer of Cr/Au (Figure 2 a, b). The application of an AC field (120 KHz, 5 V peak-to-peak for a duration of 60–75 s) between the silicon core and the Cr/Au layer generates a dielectrophoretic force strong enough to attract nucleic acids at the DENT tip (Figure 2 c,d)^[23]. When this procedure is performed within the cytoplasm of a living cells, nucleic acids can be extracted from the cell and deposited in a PCR tube for further analysis (Figure 2 e). The integration of DENT with a conventional AFM setup enables the precise positioning of the nanoprobe with nm resolution within the cytoplasm of a living cell. Also, the nanometer-sized probe minimizes the mechanical disruption to the cell membrane thus allowing high cell viability “post-surgery”. Functionalisation of the DENT with gene specific-primers enabled the enrichment of specific populations of mRNAs which were then released from the tip after immersion in ice-cooled de-ionized water for 45 min.

The authors employed qPCR to confirm the success of the extraction, although a control experiment where no AC voltage was applied also showed a signal for β -actin mRNA. These results could indicate the non-specific RNA adsorption on the DENT tip and/or contamination from cell debris present in the growth media. In their 2009 paper, the authors did not investigate the reproducibility of their procedure nevertheless their seminal work paved the way for the extraction of contents from living cells.

Two years later the same group produced remarkably similar data, when they again showed via qPCR the extraction of β -actin mRNA with and without the application of the AC voltage^[24]. Also, they showed the selective extraction of mRNA oncogene from transfected cells again without any discussion about reproducibility or selectivity.

In 2017, the same group demonstrated the integration of DENT with microfluidics technology, a key step to increase the analytical throughput^[25].

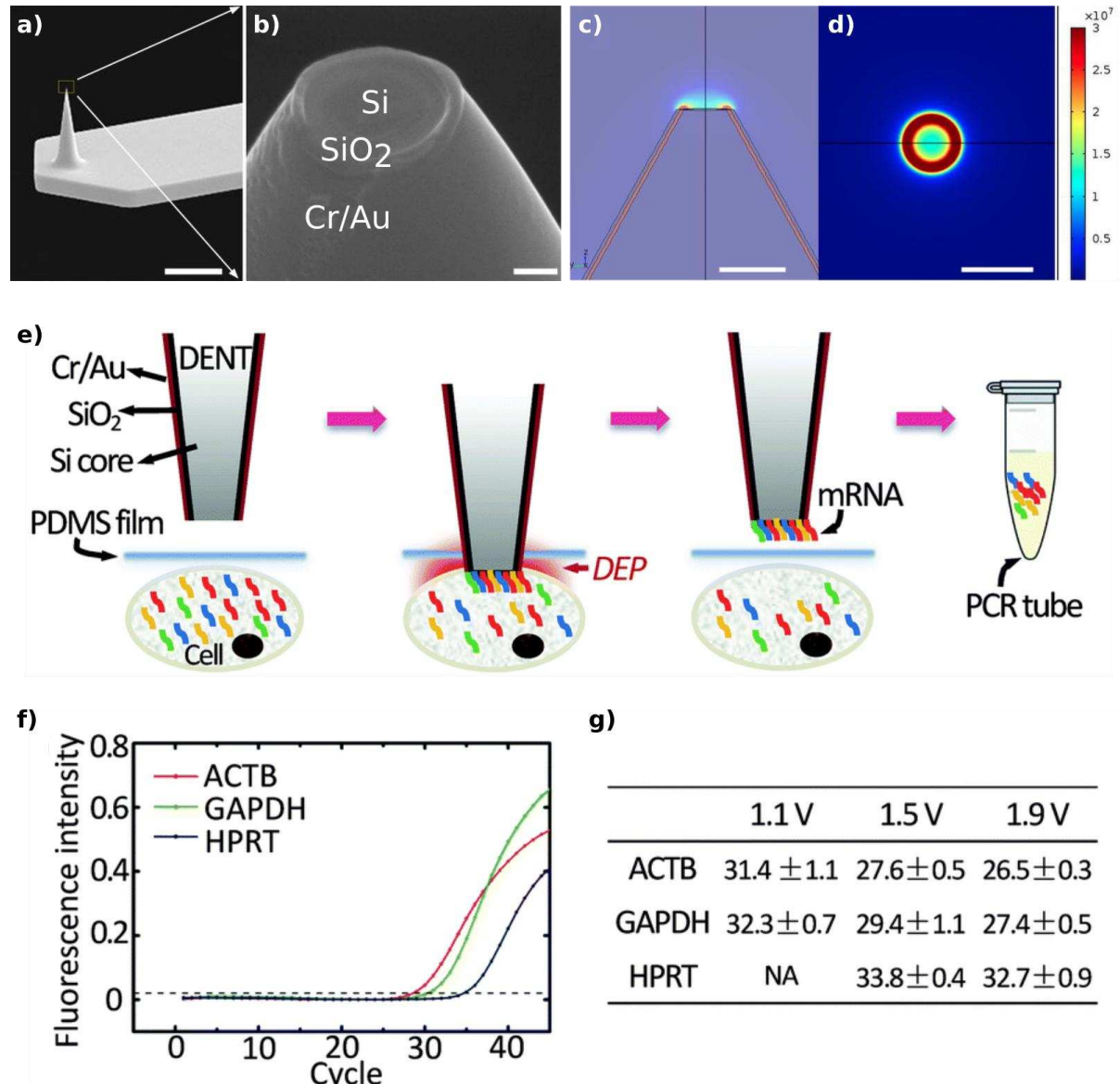


Figure 2. SEM micrographs of a) AFM cantilever (scale bar: 10 μm) and b) tip of the DENT nanoprobe composed of a highly-doped silicon core, an insulating layer of SiO_2 and a thin layer of Cr/Au (scale bar: 100 nm). Side (c) and top (d) views of the finite element electrostatic simulations of the distribution of the electric field of a DENT nanoprobe. The Si core was held at 5 Vpp at 10 MHz while the outer Cr/Au layer was grounded (scale bar: 1 μm). e) Schematic representation of nucleic acid sampling from a living cells with a DENT nanoprobe. F) RT-

qPCR graphs of three housekeeping genes' mRNAs extracted from a single HeLa cell (AC field: 1.5 Vpp, 10 MHz) (G) quantified Ct values of extracted mRNA molecules of 3 target genes (ACTB, GAPDH, and HPRT) from single HeLa cells with increasing AC voltages (1.1, 1.5 and 1.9 Vpp), with a constant frequency of 10 MHz.

The authors demonstrated that DENT nanoprobe are able to penetrate a very thinly sealed (1 μ m) microfluidic chip and isolate mRNAs from HeLa cells as well as Circulating Tumour Cells (CTCs). In this paper, they presented a more comprehensive study of mRNA isolation via qPCR analysis (Figure 2f) and they investigated the effect of varying the magnitude of the AC voltage on the efficiency of the nucleic acid isolation demonstrating that a higher AC voltage enables the isolation of a larger number of RNA transcripts (Figure 2g).

The authors noted that the amount of mRNA extracted was much lower compared to their previous work. The authors explained this result arguing that cells in the microfluidic chip were in close contact with the sealing PDMS film thus avoiding any false-positive readings and cross-contamination from cell debris in solution.

Wickramasinghe's group pioneered the application of dielectrophoretic nanotweezers for sampling from a living cell and their 2017 paper fully confirmed their potential for the selective extraction of mRNA.

1.2 FluidFM

An alternative method to extract contents from living cells using AFM technology is based on the so-called FluidFM. FluidFM combines a nanoscale tip, the force-controlled positioning of a standard AFM and a pressure-driven microchannel connected to the AFM tip as shown in Figure 3 a,b ^[26].

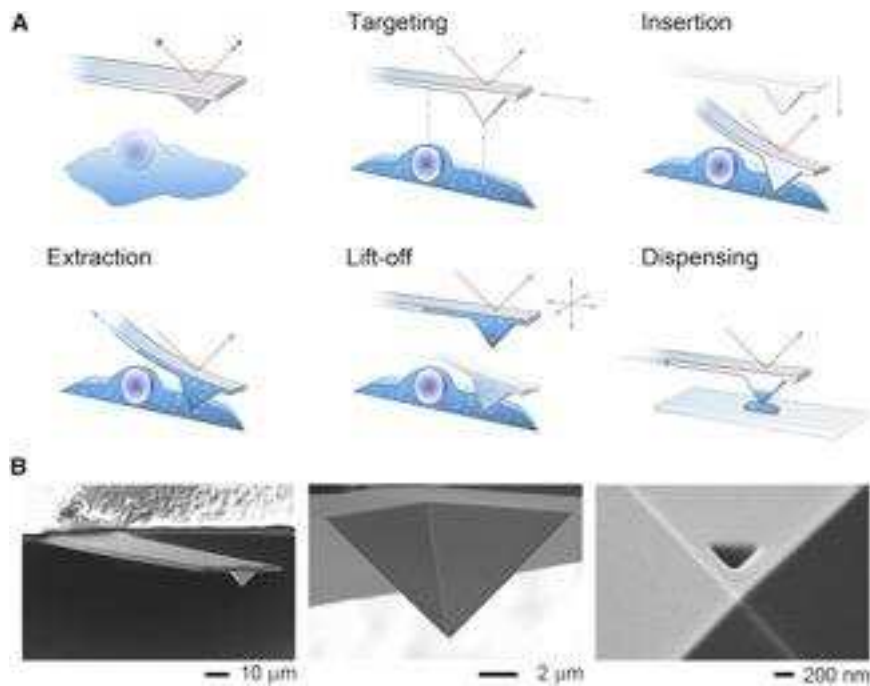


Figure 3. Schematic Representation of the FluidFM technology. A) The setup consists of an AFM mounted on top of an inverted microscope and a microfluidic nanoprobe connected to a pressure controller. Optical, force, and pressure-monitoring are performed simultaneously along the entire process B) SEM micrographs of a FluidFM tip with the fluidic aperture milled by focused ion beam on the front of the pyramidal tip. Reprinted with permission from Elsevier^[14]

In 2016, Guillaume-Gentil and co-workers published a seminal paper that demonstrated the extraction of cellular contents using the FluidFM technology combined with subsequent molecular and structural analysis of the extracted material^[14]. As with the DENT technology, the integration with the AFM force-controlled feedback mechanism allowed the precise positioning and penetration of the cell of interest. Cell contents were extracted via the application of a negative pressure to the microchannel connected to the FluidFM tip.

Arguably, this study was the most comprehensive work published to date demonstrating extraction from within a single living cells and subsequent molecular analyses. Guillaume-Gentil et al. demonstrated selective nuclear and cytoplasmic extraction by first labelling the

cell nuclei with a fluorescent protein (mRuby) tagged with a nuclear localization sequence (NLS). While mRuby has a size similar to the GFP protein, the NLS-tag leads to the active import of the reporter protein into the cell nucleus. Following insertion of the FluidFM tip and extraction directly from the nucleus, a decrease in fluorescence was observed, whereas no decrease in fluorescence was detected when the same procedure was performed in the cytoplasm. To demonstrate selective cytoplasmic aspiration, the team used the FluidFM to inject the cell nuclei with a 70 kDa dextran-conjugated fluorophore (fluorescein isothiocyanate [FITC]-dextran), which is unable to cross the nuclear pores without active transport. The authors measured a decrease in FITC fluorescence following extraction from the nucleus, whereas no noticeable change was detected when the same procedure was performed in the cytoplasm. These results indicated that the two fluorescent markers remained confined and were selectively extracted from the nucleus. In the same paper the authors monitored optically the aspirated volume and estimated the rate of aspiration as 0.4 ± 0.1 pl/min for both cytoplasm and nucleus extractions.

The authors also thoroughly investigated cell viability after cytoplasmic and nuclear aspirations. They concluded that cytoplasmic extraction of 4.0 pL from a cell resulted in 82% cell survival while aspirations of 4.5 pL and above resulted in 100% cell death (for reference the reported volume for a HeLa cell ranges between 1.2 and 4.3 pl [27]). This result is quite remarkable and indicates the cells have the ability to tolerate the loss of a large portion of the cytoplasm. Also 86% of the cell survived a nuclear aspiration of 0.6pL but aspiration volumes of 0.7pL and above resulted in cell death.

The authors also used the FluidFM to aspirate cellular contents followed by spotting on a Transmission Electron Microscopy (TEM) grid using overpressure (Figure 4 a, b). After staining, the contents were imaged using a TEM and showed features and structures consistent with the site of aspiration (Figure 4 c, d).

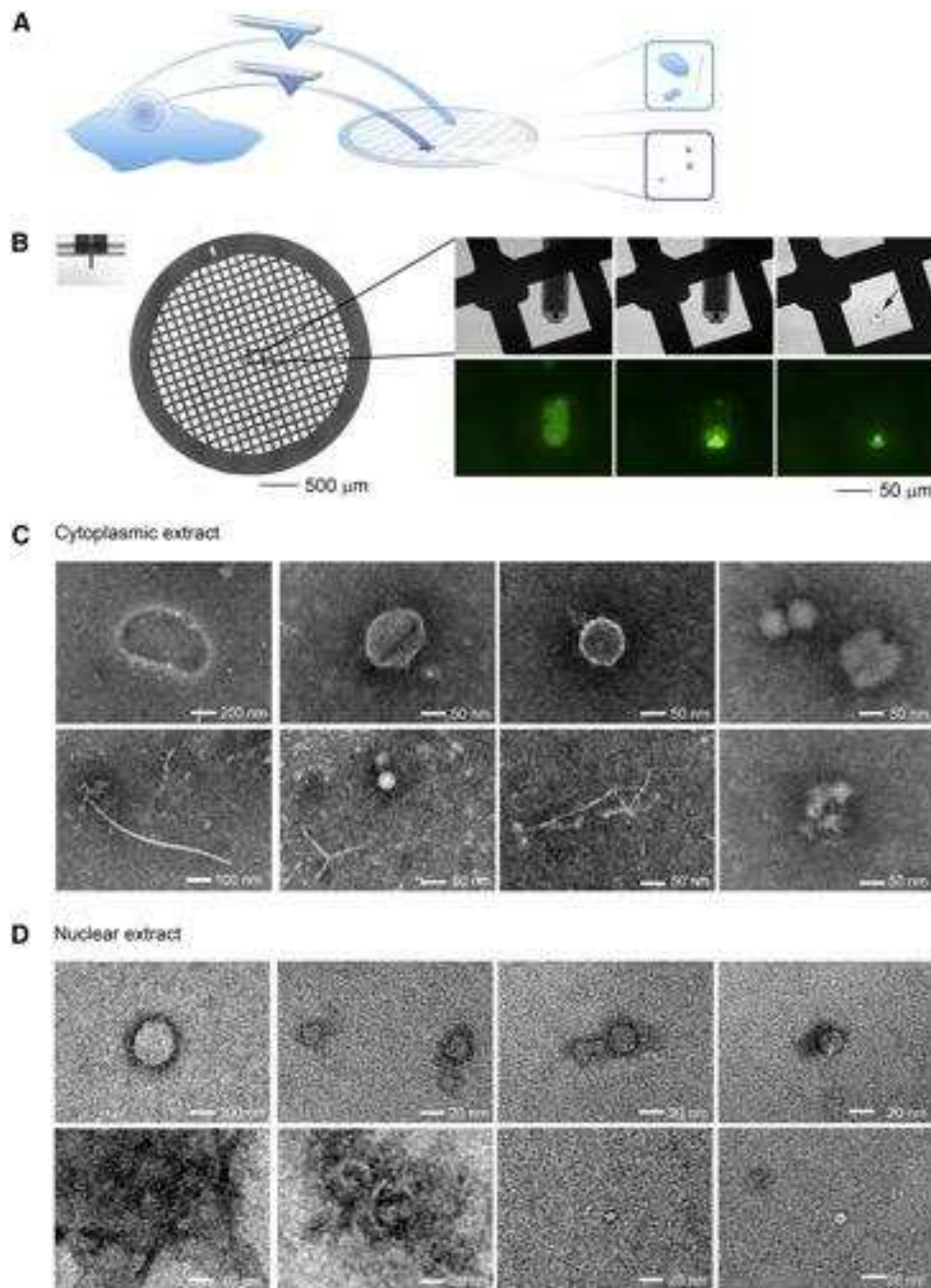


Figure 4. (A) Schematic representation of the strategy for the molecular imaging of cytoplasmic and nuclear extracts. (B) Images of the TEM grid and the FluidFM cantilever (left) zoom-in of the FluidFM spotting of the cell contents on the TEM grid (right). The phase-contrast and fluorescent micrographs demonstrate the dispensing of cell extract (arrow) on the TEM grid. Representative TEM micrographs of distinctive cellular structures observed in

negatively stained (C) cytoplasmic extracts and (D) nuclear extracts. Reprinted with permission from Elsevier ^[14].

Having demonstrated controlled aspiration of cellular contents, performed in depth cell viability studies, and analysed the aspirated nucleic acid using qPCR, the authors also validated the viability of extracted proteins using enzymatic assays. The authors then concluded the study with an in-depth analysis of extracted mRNAs from 3 different genes: two housekeeping genes and one encoding for GFP extracted from both the cytoplasm and the nucleus from HeLa cells, and GFP-transfected HeLa cells.

In a subsequent paper, the same group demonstrated that the FluidFM technology can also be used to extract contents from living cells for subsequent Matrix-Assisted Laser Desorption/Ionization Time Of Flight Mass Spectrometry (MALDI-TOF-MS) [27]. The approach was similar to the one used in their previous work^[14] but in this case the contents extracted from a living cells were spotted on a MALDI target. MALDI is an ionization technique where analytes are spotted on a solid matrix. A laser is then used to irradiate the matrix to generate high heat which triggers the analyte desorption and ionization. The ionized analytes (i.e. charged) are then driven to the detector via a potential difference between the matrix and the detector. Since the applied potential is constant, ions with smaller mass to charge ratio (m/z value) and more highly charged ions will reach the detector sooner than ions with larger m/z value (or less charged). Consequently, the time of ion flight to the detector will depend on the mass-to-charge ratio value of the ion.

Using this technique, the authors demonstrated that is possible to analyse cytoplasmic metabolites from single living cells. The authors achieved the detection of several acids and phosphorylated compounds including: ribonucleotides (cGMP, UDP, ADP, ATP), activated sugars (UDP-GlcNAc, UDP-Glc), amino acids (aspartate, glutamate), and glutathione.

The work of Guillaume Gentil and coworkers is arguably the most comprehensive study which demonstrate that methods for extracting contents from living cells and not only suitable for the extraction of nucleic acids but are also capable of sampling larger cellular structure which can then be further analyse with electron microscopy. Remarkably, they have also demonstrated the potential of FluidFM as a tool for single-cell proteomics and metabolomics^[10].

2. SICM-based Methods

2.1 Nanobiopsy

An alternative method per the extraction of contents from living cells relies on nanopipettes integrated in a Scanning Ion Conductance Microscope (SICM). SICM is a scanning probe technique that monitors the magnitude of the ion current through a nanopipette to reconstruct the topography of a sample in solution. A nanopipette is a very fine glass needle with a typical pore diameter of 100nm that can easily and reproducibly fabricated without the need for clean-room facilities (Figure 5a). Since SICM only works in solution and the feedback mechanism is force-free, it has been very successfully applied for the imaging of living cells for well over 20 years^[28, 29]. In 2014, Actis and coworkers demonstrated that SICM technology can extract RNA and organelles from within living cells without affecting their viability^[13].

Rather than using a negative pressure as with FluidFM or dielectrophoretic force as with the DENT, the authors employed elettrowetting within a nanopipette to extract minuscule amount of cytoplasmic material for analysis. Electrowetting is a physical effect where an applied voltage is used to modify the surface tension of a liquid. When a nanopipette is filled with an organic solution (i.e. dichloroethane) and it is immersed in an aqueous solution a liquid-liquid interface forms at the tip of the nanopipette due to the immiscible nature of the two liquids. Upon application of a small (300 mV) voltage to the electrode fitted inside the nanopipette, aqueous solution can be drawn inside the nanopipette tip. If this procedure is performed within a living cell than cellular contents can be aspirated in the nanopipette tip. The volume aspirated

depends, other than on the geometry of the nanopipette tip, on the magnitude and duration of the applied voltage and scientists reported that attolitre resolution (10^{-18} L) could be obtained with this method^[30].

Similarly to the DENT and FluidFM technology, the integration with scanning probe microscopy enables the precise positioning of the nanopipette with nm resolution with respect to the membrane of the cell of interest. The membrane can then be penetrated by a predefined distance and the electrowetting procedure provides a very sensitive (in the fL range) and quick (few seconds) method to manipulate ultra-low volumes within the cytoplasm of a living cell.

The authors used this method to extract minute amounts of mRNA from human fibroblasts that were then analysed with next-generation DNA sequencing.

The sequencing data of the most abundant transcripts sampled via nanobiopsy demonstrated that full-length RNA can be extracted from a single living cell and that the procedure is compatible with the sample preparation techniques used for next-generation DNA sequencing.

In the same paper, the authors demonstrated that the nanobiopsy platform is capable of extracting mitochondria from different locations of a single living cell without affecting its viability. Mitochondria are cell organelles whose predominant role is ATP production and to regulate cellular metabolism^[31]. The mitochondrion has its own independent genome and since most eukaryotic cells contain many hundreds of copies of mitochondrial DNA, the presence of more than one organellar genome within a cell is very common, which is designated as mitochondrial heteroplasmy^[32].

Figure 5 b) shows a fluorescent image of human fibroblasts whose mitochondria have been stained with a green dye before (left panel) and after (right panel) nanobiopsy. The red circle highlights the area when the biopsy took place where a diminished fluorescence intensity can be seen. Also in figure 5 c) the left panel is an optical micrograph of the nanopipette tip after mitochondria biopsy and the right panel is the inverted fluorescent image (black areas indicate

high fluorescence) that shows high fluorescence at the nanopipette tip suggesting successful mitochondria aspiration.

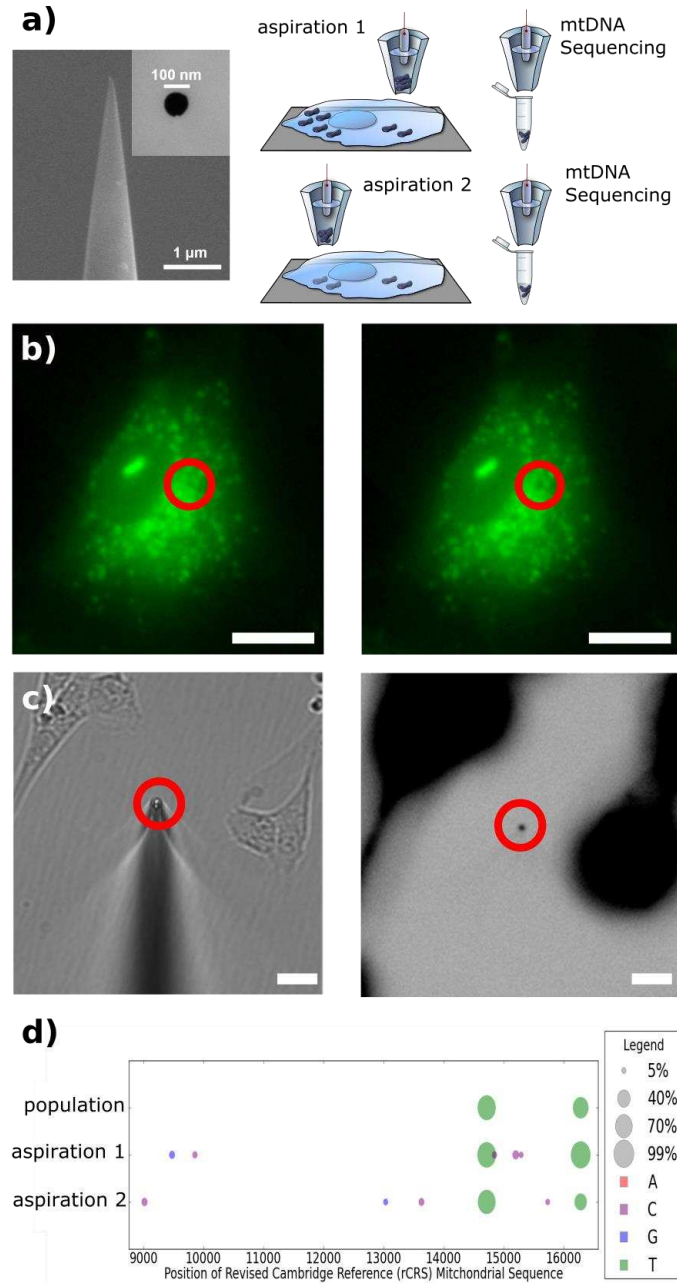


Figure 5. Mitochondrial nanobiopsy. (a) SEM micrograph of the nanopipette tip and opening and schematic representation of the nanobiopsy platform applied to the sampling of mitochondria (b) Fluorescent micrograph of human BJ fibroblast cells whose mitochondria

were labelled with MitoTracker Green before nanobiopsy (right panel) and after nanobiopsy (left panel). Red circles highlight the darker area following the sampling of mitochondria. Scale bars 15 μm . (c) (left panel) Bright-field image of the nanopipette tip (red circle) used for mitochondria nanobiopsy in panel a. (Right panel) Negative fluorescent micrograph (black areas indicate high fluorescence) of left panel showing fluorescence at the nanopipette tip which indicates successful mitochondria extraction. Scale bars 15 μm . (d) Mitochondrial sequencing results demonstrate variable conservation of heteroplasmic frequencies in aspirations. Heteroplasmic variants with estimated frequencies between 5% and 99% are displayed as circles where the area of the circle is proportional to the observed frequency. The colour of the circles specifies the nucleotide of the variant (A is red, C is violet, G is blue, and T is green). Adapted with permission from Actis et al ^[13]. Copyright 2014 American Chemical Society

The authors performed mitochondrial DNA sequencing from two mitochondrial populations extracted from different locations within the same cell and compared the results with a population-based analysis (Figure 5 D). The 14713 A→T variant shows similar frequencies across aspirations and population; whereas the 16278 C→T variant shows a greater variance of heteroplasmic frequencies in aspirations. Also, low frequency variants were found in both aspirations but not in the population analysis. These results demonstrated that only using nanobiopsy technology low heteroplasmic variants were observable.

This study was not as comprehensive as the one published by Guillaume-Gentil et al but demonstrated that the contents extracted from a single living cells can be analysed using next-generation sequencing technology and that the nanobiopsy technology can be employed for sampling organelles from living cells.

One of the implicit advantage of integrating nanoprobe with scanning probe microscopies is the ability to use the feedback mechanism to precisely position the nanoprobe with nm-resolution in the three dimensions. All the methods discussed so far only took advantage of z-resolution, but building upon the nanobiopsy work, Nashimoto and co-workers employed dual-barrel nanopipettes to demonstrate high resolution topographical mapping of the cell of interest followed by sampling^[33].

Nashimoto and coworkers observed that the ion current obtained from a DCE filled nanopipette was not sufficient to provide precise x-y positioning. To solve the issue, they employed a dual barrel nanopipette, where one barrel was filled with an aqueous solution for topographical mapping of a living cell and the second barrel was used for electrowetting-driven cell sampling. With this technique, they managed to study mRNA localization in single mouse fibroblast cells and to determine the cellular differentiation status of mouse embryo bodies (Figure 6).

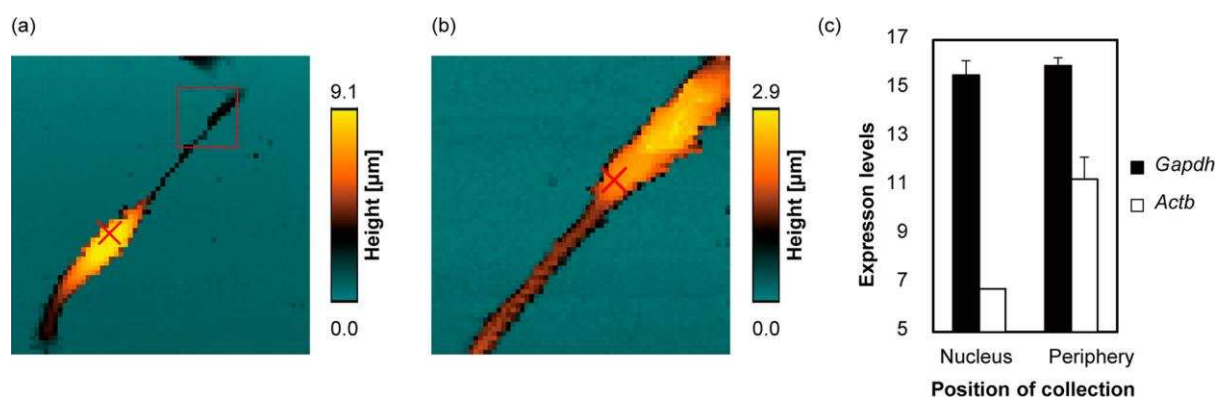


Figure 6. Nanoscale topography imaging and RNA sampling. (a) Representative SICM image ($100 \times 100 \mu\text{m}$) (b) Close-up image ($20 \times 20 \mu\text{m}$) of the of the red square in (a). The red crosses indicate the location where cytoplasmic samples were (c) mRNA expression levels for two housekeeping genes for each sampled location. mRNA expression levels were defined as 35-Ct where Ct indicates threshold cycle number. Reprinted with permission from Nashimoto et al ^[33]. Copyright 2016 American Chemical Society

2.2 Nanopipette aspiration

Baker's group also employed nanopipettes but coupled with pressure-driven sampling to probe single *Allium cepa* (Onion) cells and live *Drosophila Melanogaster* first instar larvae^[16]. The authors also performed lipid analyses from mouse brain tissue sections with a 50 μm spatial resolution.

In this study, the authors first characterized the volume aspirated as a function of the pressure applied to the nanopipette and nanopipette geometry. The authors concluded that the aspiration volume is linearly correlated with the applied pressure within the nL- μL range for nanopipettes with inner diameter larger than 200 nm. For nanopipettes smaller than 200nm the authors observed a non-linear correlation between applied pressured and volume sample and attributed the non-linearity to the length of the nanopipette shank. The authors established that liquid manipulation in the low nL range required nanopipettes with 150-nm shank.

The authors then used a 600nm nanopipette to sample approximately 8 nL of the cytoplasm of *A. cepa* cells which was then analysed with MALDI-MS (Figure 7 a). The peaks obtained in the MS spectra were attributed to hexose-oligosaccharides which were observed as potassium adducts since onion bulbs contain high level of potassium (Figure 7 b).

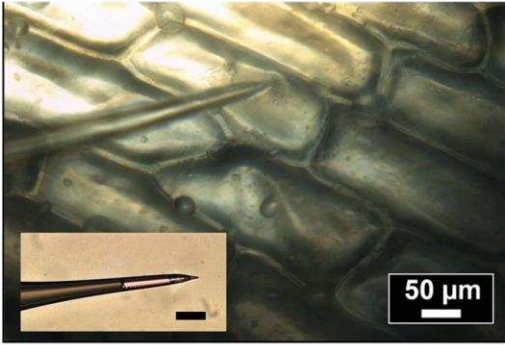
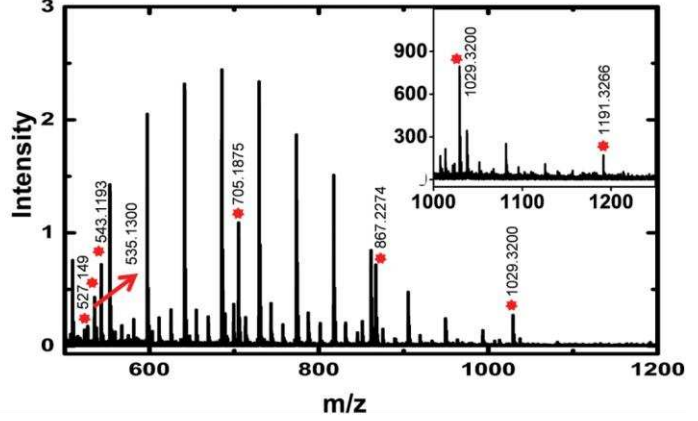
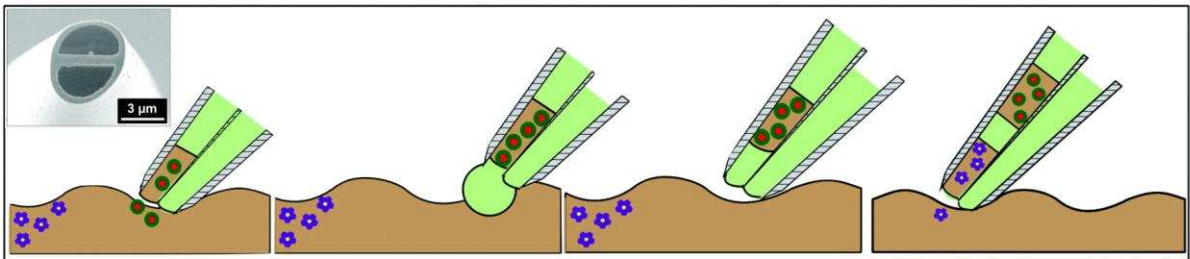
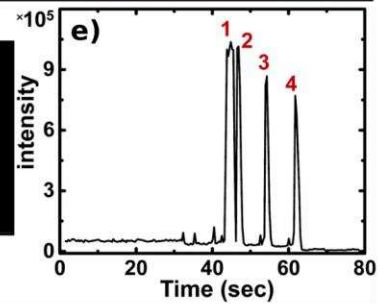
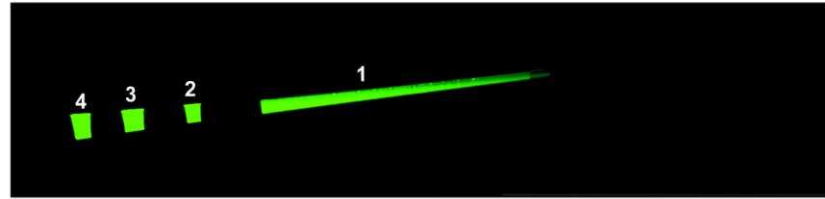
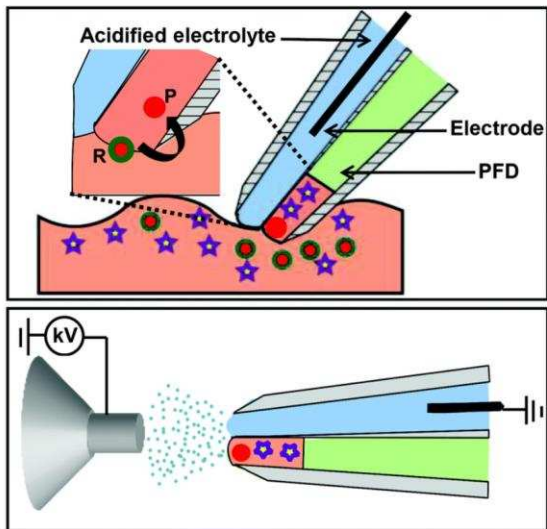
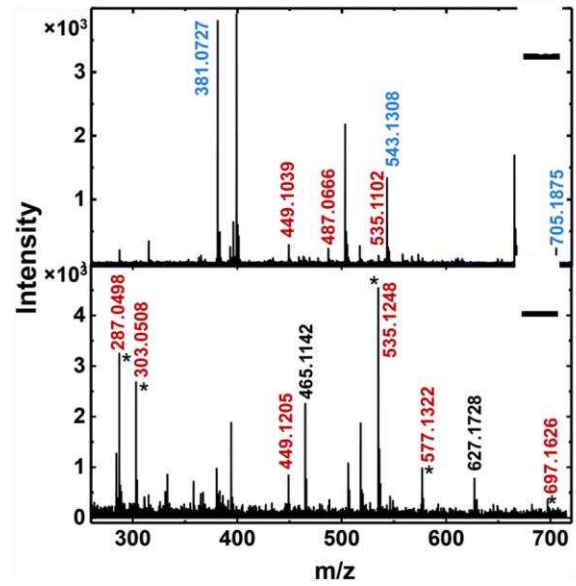
a)**b)****c)****d)****f)****g)**

Figure 7. (a) Optical micrograph showing the nanopipette sampling a single *A. cepa* epidermal cell. Inset: optical micrograph of the nanopipette after sampling (scale bar: 50 μm). (b) Positive ion MALDI-TOF mass spectrum of the sample extracted from a. The red asterisks mark peaks attributed to metabolites from the cells while the high intensity peaks correspond to the internal calibrant. (c) Schematic representation of the steps involved in segmented flow sampling with a dual-barrel nanopipette. Inset shows a SEM micrograph of a dual-barrel nanopipette. (d) Fluorescence micrograph of a nanopipette featuring 4 segmented samples of disodium fluorescein. (e) Extracted ion chromatogram (EIC) from the segments shown in (d). (f) Schematic representation of e) sampling and chemical reaction within the acidified electrolyte barrel and direct electrospraying of the sampled content to the vacuum inlet of a mass spectrometer. (g) Mass spectra of a single red *Allium Cepa* cell before (top panel) and after (lower panel) acid-catalysed degradation of oligosaccharides. Peaks marked with a star showed significant enhancement upon chemical degradation. The peaks labelled in red are anthocyanins, in blue are oligosaccharides, and flavonoids are in black. Adapted from Saha-Shah et al^[16, 34, 35] with permission from the Royal Society of Chemistry.

To demonstrate the versatility of the technique for sampling complex biological samples, the authors sampled the haemolymph of first instar *D. melanogaster* and mouse brain tissue and analysed the extracted content with MALDI-MS. The article very interestingly expanded the range of application of sampling technologies to plant cells, tissue slices and larvae and also demonstrated that is fully compatible with state of the art mass spectrometry techniques.

Baker's group also developed a method for the segmented flow sampling using double barrel nanopipettes. Segmented flow sampling was achieved by filling both barrels of a dual-barrel nanopipette with perfluorodecalin (PFD). The dual barrel nanopipette was first inserted into the cytoplasm of *Allium Cepa* cell. Negative pressure on barrel 1 causes influx of cytoplasmic

content. Positive pressure from barrel 2 causes formation of an outward PFD meniscus than is then aspirated in barrel 1 thanks to the application of a negative pressure^[34]. This procedure can then be repeated to create segment of sampled content sandwiched between immiscible PFD layers as shown in Figure 7 c, d.

The sampled content can then be directly “electrosprayed” to the vacuum inlet of the mass spectrometer without any transfer step (Figure 7f). The authors are still investigating the mechanism of electrospraying from nanopipettes but indicated that a stable electrospray was routinely achieved during MS analysis. Also in a subsequent publication, the same group demonstrated that this method can also be used for the enrichment of specific oligosaccharide via acid treatment within the nanopipette barrel^[35]. The top panel of Figure 7g shows the mass spectrum following the sampling from an *Allium Cepa* cell in a nanopipette barrel filled with ultrapure water while the bottom panel shows the sampling into a methanol–water–acetic acid (70:30:0.1) solution which induced an acid-catalysed degradation of oligosaccharides.

Nanostraws

An alternative approach to nanoprobe-based methods for extracting material from living cells relies on nanostraws protruding from a polycarbonate membrane (Figure 8 a, b) ^[36].

Nanostraws are 150-nm wide, 1 μm long cylindrical channels that are fabricated starting from commercially available track-etched polycarbonate membrane. A thin layer of Al_2O_3 is deposited on the membrane including the track etched tracks which will become the nanostraw walls after careful etching. Photolithography is then used to define a precise sampling region within the 1 μm - 1mm range (Figure 8 c, d, e, f).

Cells of interest can be cultured directly on the nanostraws-embedded substrate and in several studies Melosh’s group demonstrated that nanostraws indeed penetrate the cell membrane and provide direct fluidic intracellular access ^[37-39]. In particular, the group found that NS with a

diameter of 100 nm or smaller spontaneously penetrate the cell membrane, allowing the delivery of small molecules into cells while nanostraws with a diameter of 150 nm and above are engulfed by the cell without causing membrane rupture.

Cao et al demonstrated that the nanostraws platform is suitable for the longitudinal studies of few cells (20/30 cells) but it can also be applied to single-cell sampling.

The authors employed 150-nm wide nanostraws that were engulfed by the cells but did not provide a continuous fluidic intracellular access. Cytoplasmic access could be gained temporary (2-5 minutes) thanks to the application of short electric pulses (10-35V) that cause membrane poration and enable fluidic access. The authors demonstrated the feasibility of this approach by longitudinally sampling GFP and RFP from CHO cells (38 cells were sampled simultaneously) and confirming the successful extraction with fluorescence microscopy while maintaining cell viability post-sampling of 95%. The authors also reduced the sampling window to 100 μm x 100 μm which allowed the sampling from a single CHO cell expressing RFP.

The authors also demonstrated that the nanostraws platform is suitable for sampling cells derived in vitro from human induced pluripotent stem cells, cells that are notoriously delicate while being an invaluable resource for drug discovery, disease modelling and cell therapy^[40].

To demonstrate longitudinal sampling the authors employed an enzyme linked immunosorbent assay (ELISA) to track the change in intracellular concentration of non-fluorescent heat-shock protein 27 (HSP27) from hiPSC-derived cardiomyocytes (hiPSCCMs) upon exposure to heat shock (44°C for 30 minutes).

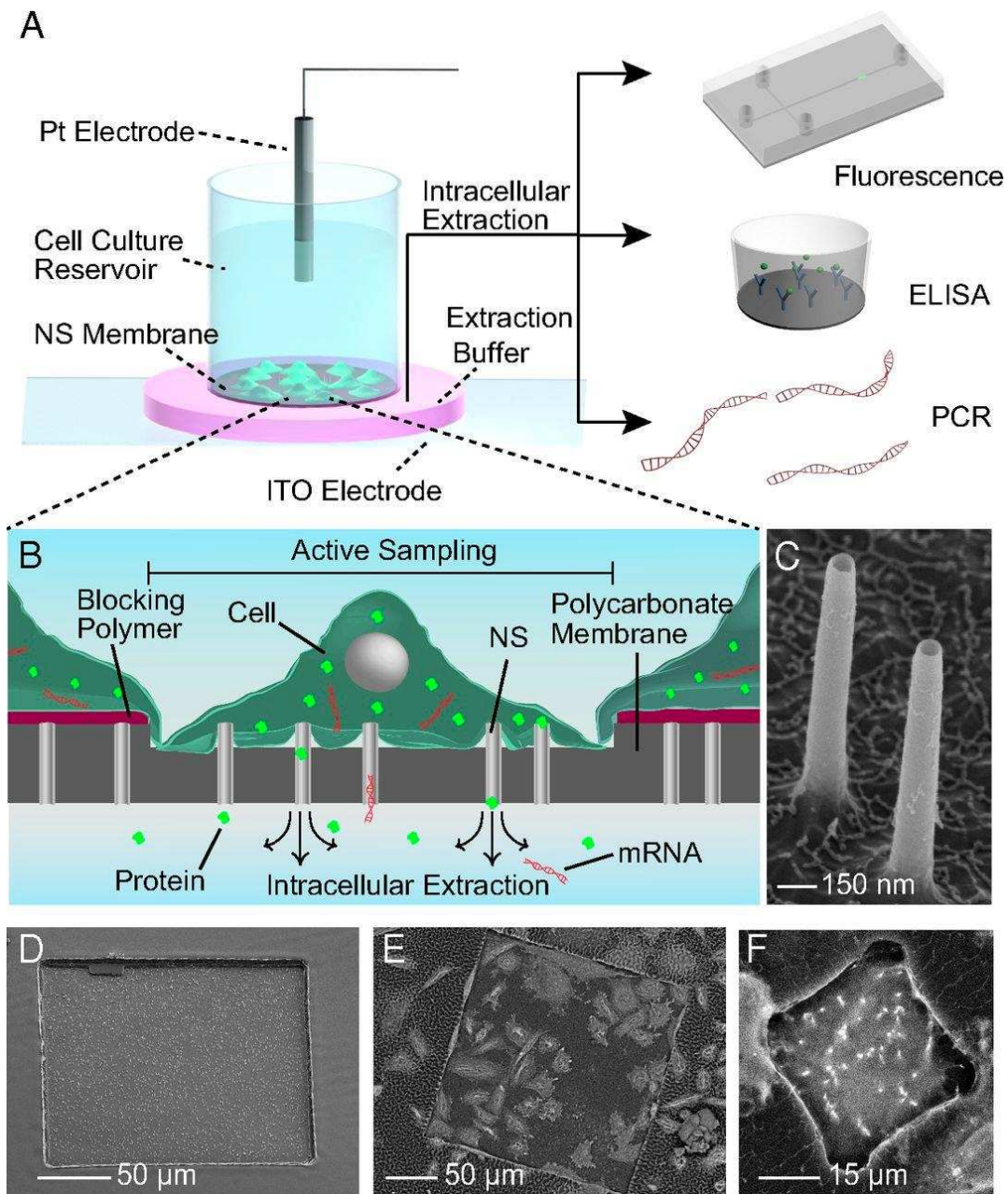


Figure 8. Schematic Representation of the nanostraws sampling platform. (A and B) The platform is based on a polycarbonate membrane with protruding 150-nm diameter nanostraws supported on a cell-culture dish. Sampling is performed by application of short voltage pulses that temporarily electroporate the cells, allowing cellular content to diffuse through the NS and into the underlying fluidic reservoir (highlighted in pink) which is then analysed using fluorescence imaging, ELISA, or qPCR. (C) SEM micrographs of the 150-nm-diameter NS and (D) the 200×200 μm active sampling region. Cells outside this window are unaffected by the sampling process. (E) SEM micrographs of cells cultured on a 200×200 μm active sampling

region containing 42 cells and (F) a 30×30 μm sampling region used to isolate and sample from a single cell.

Moreover, the authors employed the nanostraws platform to track mRNA expression from living hiPSCCMs for 3 days. Currently the sensitivity of mRNA sequencing systems is not able to measure nanostraws extractions from single cells, instead requiring approximately 15–20 cells.

This article for the first time demonstrate longitudinal sampling from living cells and this technology can sample cells in parallel rather than sequentially as with the scanning probe-based methods.

Conclusion and Perspectives

This review highlighted the creative applications of nanoprobe-based methods for extracting the content of living cells without affecting their viability. These methods can be essentially divided in two classes:

1. Mobile nanoprobe
2. Static nanoprobe

The mobile nanoprobe techniques such as DENT, FluidFM, and nanopipettes enable the precise positioning of the nanoprobe with respect of the cell of interest. These methods are generally integrated with nanomanipulators which allow automated positioning with nanoscale resolution. Cells to be analysed can be cultured in “standard” environments such as Petri dishes and these methods could also be amenable to the study of tissue slices and 3D cell cultures. However, since the sampling has to be performed in a serial fashion these methods generally lack of throughput.

Instead, the static nanoprobe methods such as nanostraws technology enables higher throughput studies because of the ability to lithographically pattern sampling areas on the

polycarbonate membrane. Cells, however, need to be grown on the nanostraws substrate which could prove difficult for tissue slices or 3D cell cultures.

The precise control over the amount of contents (or volume) extracted from a single cell is a fundamental requirement to enable quantitative longitudinal sampling. This condition requires the precise manipulation of liquids with sub pL resolution which is not trivial. Guillaume-Gentil et al took advantage of the semitransparency of the FluidFM cantilevers to visualize and quantify the extracted volume with 100fL resolution^[14]. Actis et al also attempted to estimate the volume aspirated with the nanobiopsy platform but only when aspirating from a buffer solution and never while attempting a cell biopsy^[13]. Nevertheless, Laforge et al analytically derived an equation that correlates the nanopipette resistance with the amount of aqueous solution drawn in the nanopipette during electrowetting which, in principle, could be used to monitor the volume aspirated during nanobiopsy^[30]. With the nanostraws technology, Cao et al estimated the extracted GFP by measuring the difference in fluorescence intensity from cells before and after sampling^[36]. Similarly, Li et al used qPCR to correlate the voltage applied to the DENT nanoprobes with the amount of nucleic acids extracted^[41]. Despite all these efforts for the accurate volume control during sampling, more work is needed to achieve the accuracy necessary to move away from proof-of-concept studies and start tackling fundamental biological questions.

Also, sub-cellular sampling opens up the question is the extracted sample is representative of the cell. It is very likely that a 1-10% cytoplasmic subsample will not be truly representative of the cytoplasm because sub-cellular localization of RNA is known to occur^[42]. However, techniques that visualise transcripts in situ, indicate that such localization does not occur for all transcripts within a cell, and the methods described in this review have the ability to study whether transcripts relevant to biological process (e.g drug treatment resistance) are localized and if so how this localization changes over time. Subcellular localization will of course add

to noise within the system making true signal harder to distinguish but not impossible as long as a careful power analysis is implemented.

Furthermore, the nanopipettes used for nanobiopsy experiments are fundamentally ultra-sharp patch-clamp electrodes. Recent studies demonstrated that automated patch-clamp can be performed in-vivo^[43] indicating that nanopipette-based techniques can be employed for in-vivo single-cell sampling.

A fundamental question that needs to be asked is why do we need to extract contents from living cells? It can be argued that the interest lays in the information carried by these contents more on the contents per se. Recently, optical methods for in-situ RNA sequencing with sub-cellular resolution have been reported ^[44, 45] which enabled the high throughput study of the spatial organization of RNA transcripts both in cultured cells and in tissue slices. Although these methods have not been discussed in this review, they hold tremendous potential for “sampling” information from cells and tissue with nanoscale resolution.

However, physically extracting contents from a single living cells still holds some key advantages. It allows the downstream analysis of the extracted content with large analytical tools such as electron microscopy or mass spectrometry while preserving cell viability and spatial information. Also, it could enable “single-cell transplantation” where content from cell A are transferred into cell B or, organelles transfer from cell to cell as a model to study the evolution of eukaryotic cells^[46]. The ability to physically extract contents underlies the ability of perturbing a single cell by injecting foreign material. All the methods described in this review except for the DENT technology have been used for the introduction of foreign material in cells^[26, 38, 47] and perturbation coupled with single-cell sampling is another frontier of this technologies, also considering the enormous potential for gene editing enabled by CRISPR^[48].

References

1. A. Giladi; I. Amit, *Nature* **2017**, *547* (7661), 27-29.
2. J. S. Marcus; W. F. Anderson; S. R. Quake, *Anal Chem* **2006**, *78* (9), 3084-9.
3. I. C. Macaulay; W. Haerty; P. Kumar; Y. I. Li; T. X. Hu; M. J. Teng; M. Goolam; N. Saurat; P. Coupland; L. M. Shirley; M. Smith; N. Van der Aa; R. Banerjee; P. D. Ellis; M. A. Quail; H. P. Swerdlow; M. Zernicka-Goetz; F. J. Livesey; C. P. Ponting; T. Voet, *Nat Methods* **2015**, *12* (6), 519-22.
4. S. Picelli; A. K. Bjorklund; O. R. Faridani; S. Sagasser; G. Winberg; R. Sandberg, *Nat Methods* **2013**, *10* (11), 1096-8.
5. M. Stoeckius; C. Hafemeister; W. Stephenson; B. Houck-Loomis; P. K. Chattopadhyay; H. Swerdlow; R. Satija; P. Smibert, *Nat Methods* **2017**.
6. C. Gawad; W. Koh; S. R. Quake, *Nat Rev Genet* **2016**, *17* (3), 175-88.
7. K. Shekhar; S. W. Lapan; I. E. Whitney; N. M. Tran; E. Z. Macosko; M. Kowalczyk; X. Adiconis; J. Z. Levin; J. Nemes; M. Goldman; S. A. McCarroll; C. L. Cepko; A. Regev; J. R. Sanes, *Cell* **2016**, *166* (5), 1308-+.
8. C. Ziegenhain; B. Vieth; S. Parekh; B. Reinius; A. Guillaumet-Adkins; M. Smets; H. Leonhardt; H. Heyn; I. Hellmann; W. Enard, *Mol Cell* **2017**, *65* (4), 631-+.
9. S. T. Aviv Regev, Eric S. Lander, Ido Amit, Christophe Benoist, Ewan Birney, Bernd Bodenmiller, Peter Campbell, Piero Carninci, Menna Clatworthy, Hans Clevers, Bart Deplancke, Ian Dunham, James Eberwine, Roland Eils, Wolfgang Enard, Andrew Farmer, Lars Fugger, Berthold Gottgens, Nir Hacohen, Muzlifah Haniffa, Martin Hemberg, Seung K. Kim, Paul Klenerman, Arnold Kriegstein, Ed Lein, Sten Linnarsson, Joakim Lundberg, Partha Majumder, John Marioni, Miriam Merad, Musa Mhlanga, Martijn Nawijn, Mihai Netea, Garry Nolan, Dana Pe'er, Anthony Philipakis, Chris P. Ponting, Stephen R. Quake, Wolf Reik, Orit Rozenblatt-Rosen, Joshua R. Sanes, Rahul Satija, Ton Shumacher, Alex K. Shalek, Ehud Shapiro, Padmanee Sharma, Jay Shin, Oliver Stegle, Michael Stratton, Michael J. T. Stubbington, Alexander van Oudenaarden, Allon Wagner, Fiona M. Watt, Jonathan S. Weissman, Barbara Wold, Ramnik J. Xavier, Nir Yosef, *bioRxiv* **2017**.
10. R. Zenobi, *Science* **2013**, *342* (6163), 1201-+.
11. Y. Wang; N. E. Navin, *Mol Cell* **2015**, *58* (4), 598-609.
12. O. Stegle; S. A. Teichmann; J. C. Marioni, *Nature Reviews Genetics* **2015**, *16* (3), 133-145.
13. P. Actis; M. M. Maalouf; H. J. Kim; A. Lohith; B. Vilozy; R. A. Seger; N. Pourmand, *ACS Nano* **2014**, *8* (1), 546-53.
14. O. Guillaume-Gentil; R. V. Grindberg; R. Kooger; L. Dorwling-Carter; V. Martinez; D. Ossola; M. Pilhofer; T. Zambelli; J. A. Vorholt, *Cell* **2016**, *166* (2), 506-16.
15. O. Guillaume-Gentil; T. Rey; P. Kiefer; A. J. Ibanez; R. Steinhoff; R. Bronnimann; L. Dorwling-Carter; T. Zambelli; R. Zenobi; J. A. Vorholt, *Anal Chem* **2017**, *89* (9), 5017-5023.
16. A. Saha-Shah; A. E. Weber; J. A. Karty; S. J. Ray; G. M. Hieftje; L. A. Baker, *Chem Sci* **2015**, *6* (6), 3334-3341.
17. R. Singhal; Z. Orynbayeva; R. V. Kalyana Sundaram; J. J. Niu; S. Bhattacharyya; E. A. Vitol; M. G. Schrlau; E. S. Papazoglou; G. Friedman; Y. Gogotsi, *Nat Nanotechnol* **2011**, *6* (1), 57-64.
18. Z. Yang; L. Deng; Y. Lan; X. Zhang; Z. Gao; C. W. Chu; D. Cai; Z. Ren, *Proc Natl Acad Sci U S A* **2014**, *111* (30), 10966-71.

19. R. Yan; J. H. Park; Y. Choi; C. J. Heo; S. M. Yang; L. P. Lee; P. Yang, *Nat Nanotechnol* **2011**, *7* (3), 191-6.
20. J. P. Giraldo-Vela; W. Kang; R. L. McNaughton; X. M. Zhang; B. M. Wile; A. Tsourkas; G. Bao; H. D. Espinosa, *Small* **2015**, *11* (20), 2386-2391.
21. S. G. Higgins; M. M. Stevens, *Science* **2017**, *356* (6336), 379-380.
22. D. Nawarathna; T. Turan; H. K. Wickramasinghe, *Appl Phys Lett* **2009**, *95* (8).
23. Y. L. Tao; H. K. Wickramasinghe, *Appl Phys Lett* **2017**, *110* (7).
24. D. Nawarathna; R. Chang; E. Nelson; H. K. Wickramasinghe, *Anal Biochem* **2011**, *408* (2), 342-4.
25. X. Li; Y. L. Tao; D. H. Lee; H. K. Wickramasinghe; A. P. Lee, *Lab on a Chip* **2017**, *17* (9), 1635-1644.
26. O. Guillaume-Gentil; E. Potthoff; D. Ossola; P. Dorig; T. Zambelli; J. A. Vorholt, *Small* **2013**, *9* (11), 1904-7.
27. L. Zhao; C. D. Kroenke; J. Song; D. Piwnica-Worms; J. J. H. Ackerman; J. J. Neil, *Nmr Biomed* **2008**, *21* (2), 159-164.
28. P. Novak; C. Li; A. I. Shevchuk; R. Stepanyan; M. Caldwell; S. Hughes; T. G. Smart; J. Gorelik; V. P. Ostanin; M. J. Lab; G. W. J. Moss; G. I. Frolenkov; D. Klenerman; Y. E. Korchev, *Nat Methods* **2009**, *6* (12), 935-935.
29. Y. E. Korchev; C. L. Bashford; M. Milovanovic; I. Vodyanoy; M. J. Lab, *Biophysical Journal* **1997**, *73* (2), 653-658.
30. F. O. Laforge; J. Carpino; S. A. Rotenberg; M. V. Mirkin, *P Natl Acad Sci USA* **2007**, *104* (29), 11895-11900.
31. J. R. Friedman; J. Nunnari, *Nature* **2014**, *505* (7483), 335-343.
32. Y. P. He; J. Wu; D. C. Dressman; C. Iacobuzio-Donahue; S. D. Markowitz; V. E. Velculescu; L. A. Diaz; K. W. Kinzler; B. Vogelstein; N. Papadopoulos, *Nature* **2010**, *464* (7288), 610-U175.
33. Y. Nashimoto; Y. Takahashi; Y. S. Zhou; H. Ito; H. Ida; K. Ino; T. Matsue; H. Shiku, *ACS Nano* **2016**, *10* (7), 6915-6922.
34. A. Saha-Shah; C. M. Green; D. H. Abraham; L. A. Baker, *Analyst* **2016**, *141* (6), 1958-1965.
35. A. Saha-Shah; J. A. Karty; L. A. Baker, *Analyst* **2017**, *142* (9), 1512-1518.
36. Y. H. Cao; M. Hjort; H. D. Chen; F. Birey; S. A. Leal-Ortiz; C. M. Han; J. G. Santiago; S. P. Pasca; J. C. Wu; N. A. Melosh, *P Natl Acad Sci USA* **2017**, *114* (10), E1866-E1874.
37. J. J. VanDersarl; A. M. Xu; N. A. Melosh, *Nano Letters* **2012**, *12* (8), 3881-3886.
38. X. Xie; A. M. Xu; S. Leal-Ortiz; Y. H. Cao; C. C. Garner; N. A. Melosh, *Acs Nano* **2013**, *7* (5), 4351-4358.
39. A. M. Xu; A. Aalipour; S. Leal-Ortiz; A. H. Mekhdjian; X. Xie; A. R. Dunn; C. C. Garner; N. A. Melosh, *Nature Communications* **2014**, *5*.
40. V. Tabar; L. Studer, *Nature Reviews Genetics* **2014**, *15* (2), 82-92.
41. X. Li; Y. Tao; D. H. Lee; H. K. Wickramasinghe; A. P. Lee, *Lab Chip* **2017**, *17* (9), 1635-1644.
42. N. Battich; T. Stoeger; L. Pelkmans, *Nat Meth* **2013**, *10* (11), 1127-1133.
43. S. B. Kodandaramaiah; G. T. Franzesi; B. Y. Chow; E. S. Boyden; C. R. Forest, *Nat Methods* **2012**, *9* (6), 585-7.
44. J. H. Lee; E. R. Daugharthy; J. Scheiman; R. Kalhor; J. L. Yang; T. C. Ferrante; R. Terry; S. S. Jeanty; C. Li; R. Amamoto; D. T. Peters; B. M. Turczyk; A. H. Marblestone; S. A. Inverso; A. Bernard; P. Mali; X. Rios; J. Aach; G. M. Church, *Science* **2014**, *343* (6177), 1360-3.

45. F. Chen; A. T. Wassie; A. J. Cote; A. Sinha; S. Alon; S. Asano; E. R. Daugharthy; J. B. Chang; A. Marblestone; G. M. Church; A. Raj; E. S. Boyden, *Nat Methods* **2016**, *13* (8), 679-84.
46. P. Tiefenboeck; J. A. Kim; F. Trunk; T. Eicher; E. Russo; A. Teijeira; C. Halin; J. C. Leroux, *ACS Nano* **2017**.
47. R. Adam Seger; P. Actis; C. Penfold; M. Maalouf; B. Vilozy; N. Pourmand, *Nanoscale* **2012**, *4* (19), 5843-6.
48. P. D. Hsu; E. S. Lander; F. Zhang, *Cell* **2014**, *157* (6), 1262-78.